Numerical modelling of stepped helical cooling channels

Numerical modelling of stepped helical cooling channels

M Grespan[1], D Trane[1], L Campanelli[1], D Angeli[2] and R Freddi[3]

[1] DISMI - Dipartimento di Scienze e Metodi dell'Ingegneria, Università di Modena e Reggio Emilia, Via Amendola 2, Pad. Buccola, 42122 Reggio Emilia (Italy)

E-mail: mattia.grespan@unimore.it

[2] Centro Interdipartimentale EN&TECH, Piazzale Europa 1, 42124 Reggio Emilia (Italy)

[3] Fira Spa, Strada Statale 255, 374/B, 44047 Dosso Terre del Reno, Italy

Abstract. The automotive industry is in the midst of a radical change of propulsion technology to meet the increasingly stringent limits on emissions and fuel consumption. Electric and hybrid power-trains are progressively replacing their internal combustion counterparts, as they are more efficient, especially in transient operation. In electric and hybrid vehicles effective cooling system operation is of utmost importance as it influences directly the efficiency and power density levels achievable by the power train. Thus, accurate analyses are needed to maximize the thermal performance of these systems. In this work an electric motor cooling jacket, that features a stepped helical geometry, is studied by means of CFD, with a particular focus on the head losses. The periodicity of the cooling channels geometry along the helical development is exploited to reduce the computational domain to a basic periodic module. The flow field is determined by applying a 3D Finite Volume approach, and numerical solutions are obtained by means of a validated incompressible solver. Novel boundary conditions are purposely developed to allow for the coupling of the inlet and outlet patches, which are roto-translated with respect to each other. The sensitivity of integral results on friction losses, with respect to the number of periodic modules included in the model, is investigated. The developed numerical model is employed to obtain a suitable correlation for the equivalent Darcy friction factor as a function of the Reynolds number only. Finally, a first estimation of the total head losses is obtained by using the Darcy Weisbach formula along with the aforementioned friction factor correlation.

Keywords: electric motor, cooling jacket, head losses, rototranslational mapping, CFD, RANS

1. Introduction

The progressively severe limits on fuel consumption and pollutant emissions are increasingly promoting the use of electric and hybrid powertrains instead of traditional internal combustion engines. The specific power output and efficiency levels of electric motors employed in these power units is determined by the effectiveness of the chosen cooling solution, thus its design is of critical importance. Impressive power density levels of more than 5 kW/kg can be achieved by employing water cooled motor casings [1]. The cooling channel shape must be devised in order to minimize head losses and maintain adequate heat transfer performance. Several authors dealt with the analysis of cooling jackets of electric motors, which usually, except for very simple geometries, requires the use of numerical techniques, such as Computational Fluid Dynamics (CFD). Ye *et al.* [2] studied cooling jackets with different layouts by developing CFD models of

the whole channels geometry. Similarly, Pechánek and Bouzek [3] presented a thorough analysis about cooling jackets featuring circumferential and axial channels. Nategh *et al.* [4] performed CFD analyses to determine coolant flow distribution through the cooling channels of a motor casings. Then the authors employed the resulting velocity values to compute heat transfer coefficients according to empirical correlations. A simplified approach is presented in [5], in which the authors exploited the periodicity and symmetries of the cooling jacket geometry to significantly reduce the complexity of the model, and thus the required computational resources.

This work presents the first steps in the development of a numerical model to study the internal flow inside a cooling jacket that features stepped helical cooling channels, with a particular focus on head losses. The examined motor casing is manufactured by means of a patented process in which aluminium plates having milled circumferential slots are stacked and brazed together. The result is a casing endowed with great mechanical strength and cooling channels whose shape is dictated by angular span of the slots, their position on each plate, and the height of the plates.

The intricate shape and the considerable length of the cooling channels imply that numerical fluid flow analysis of the whole domain would be a cumbersome task, due to the large computational resources that would be required. Thus, the channels are studied through periodic modules under fully developed flow conditions; these are enforced by coupling the numerical solution at the inlet and outlet sections, which share a roto-translation transformation. However, most commercially available CFD tools allow for solution coupling between mesh faces only if these are connected by simple translational or rotational transformations. To solve the problem, a new boundary condition is developed for the OpenFOAM computational library [6] in order to attain solution coupling between rototranslated mesh patches.

The newly developed computational tools are validated by performing a test CFD run to verify the correct coupling of scalar and vector fields. Subsequently, the dependence of the results with respect to the number of channel slots included in the periodic module is investigated, by comparing local and global results obtained from computational domains featuring one, two, and four slots. After the selection of the final computational model, a grid sensitivity analysis is performed, and a suitable correlation is obtained for the equivalent Darcy friction factor, which is the chosen parameter to express global results on head losses.

Finally, a first estimate of the overall pressure drop related to the cooling jacket is made using the Darcy Weisbach formula, and the previously mentioned correlation for the equivalent Darcy friction factor.

2. Case study

The aluminium motor casing examined in this work features a water cooling jacket, that includes six cooling channels which develop in steps along a cylindrical helix. This particular arrangement is achieved thanks to a patented manufacturing process which involves brazing a stack of aluminium plates that feature machined circumferential slots. The assembly of aluminum plates resulting from the brazing process is shown in Fig. 1a, while an example of a slotted plate is depicted in the drawing of Fig. 1b. Subsequent machining operations are performed to obtain the final motor casing. The geometry of the stepped helical channels is determined by the height of each plate y, the slot width x, the slot angular span β, and the angular offset between two subsequent slots α. The channels mean radius r is determined by the external diameter of the stator of the motor, and by the minimum wall thickness necessary to guarantee adequate mechanical resistance. Figure 1c shows a simple drawing depicting six helical channel steps, along with their main dimensions. The cylindrical helix formed by the succession of channel steps is identified by the following parametric equation:

$$h(\vartheta) = r\cos\vartheta\,\hat{i} + r\sin\vartheta\,\hat{j} + \left(\frac{y}{\alpha}(\vartheta - \vartheta_0) + z_0\right)\hat{k}\,, \tag{1}$$

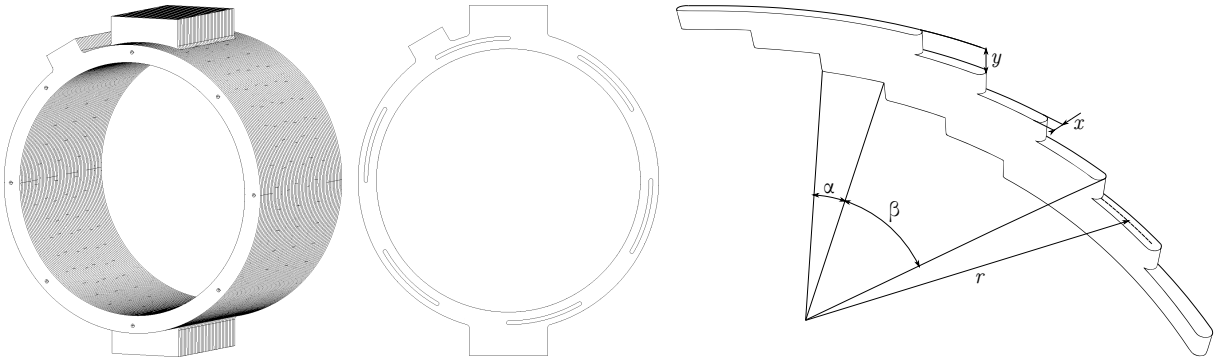

(a) (b) (c)

Figure 1. External geometry of the examined motor case as brazed (a), schematic of a slotted plate (b), and the geometry of the cooling channels along with their relevant dimensions (c).

where ϑ_0 and z_0 are arbitrary initial values which locate the helix in space.

3. Numerical methods

3.1. Governing equations

Stepped helical channels are studied by means of CFD analysis of periodic modules, under fully-developed flow conditions. In this preliminary phase, periodic modules consisting of a different number of channel steps are considered, with the aim of assessing the sensitivity of the results with respect to the number of steps. The flow about each periodic module is assumed steady and incompressible, and it is determined from the numerical solution of the RANS equations.

$$\begin{cases} \nabla \cdot (\vec{v} \otimes \vec{v}) = -\dfrac{1}{\rho} \nabla p + \nabla \cdot [(\nu + \nu_t) \nabla \vec{v}] + \sigma \\ \nabla \cdot \vec{v} = 0 \end{cases} \tag{2}$$

Closure of the RANS equations is attained by means of the k-ω SST turbulence model [7]. The external forcing σ in Eqs. (2) is iteratively determined as part of the solution to maintain the desired flow rate. The problem is addressed by means of a dimensionless framework based on the height of a single channel step y, which is designated as the reference length, and is used to scale down the computational domain. The flow is then defined solely on the basis of the Reynolds number. Mean inlet velocity and fluid density are set to unitary reference values, thus leading to the following definitions for the physical properties in Eqs. (2):

$$\mu^* = \nu^* = \frac{1}{\mathrm{Re}} \, . \tag{3}$$

3.2. Rototranslational mapping

Fully developed flow conditions are achieved by coupling the flow numerical solution at the inlet at outlet sections, each of which is defined by rototranslation of the other one. Since in most commercially available CFD tools coupling between patches is only allowed if simple translation or rotation transformations are involved, a novel boundary condition is developed for the OpenFOAM numerical suite [6]. Solution coupling between rototranslated mesh patches is achieved by means of an explicit mapping procedure: the face centres coordinates on a given patch are transported onto the neighbour one by means of a face-centre-specific offset vector:

$$\boldsymbol{o}_i = \boldsymbol{x}'_i - \boldsymbol{x}_i = (\boldsymbol{R} - \boldsymbol{I}) \, \boldsymbol{x}_i + \boldsymbol{t} \, , \tag{4}$$

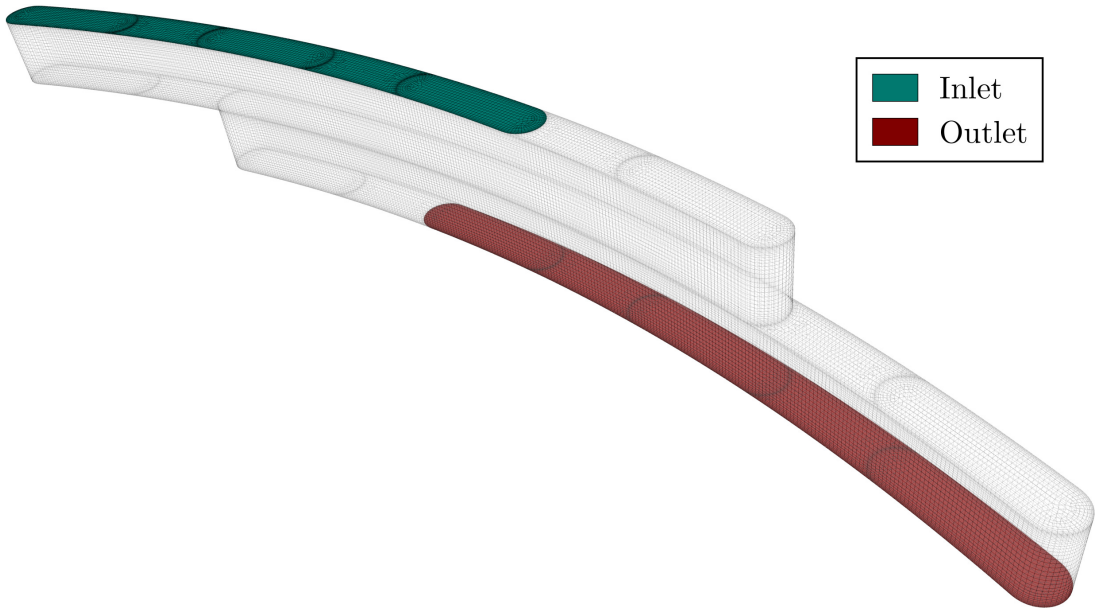

Figure 2. An example of computational grid including two helical channel steps.

where $\boldsymbol{x}_i'$ and $\boldsymbol{x}_i$ stand for the transformed and unchanged coordinates of the i-th face centre, respectively. $\boldsymbol{R}$ is a rotation matrix derived from matrix multiplication of the three transformation matrices, associated with rotations whose Euler angles are ϕ, χ, ψ about the x, y, z axes, respectively.

$$\boldsymbol{R} = \begin{bmatrix} \cos\psi & -\sin\psi & 0 \\ \sin\psi & \cos\psi & 0 \\ 0 & 0 & 1 \end{bmatrix} \begin{bmatrix} \cos\chi & 0 & \sin\chi \\ 0 & 1 & 0 \\ -\sin\chi & 0 & \cos\chi \end{bmatrix} \begin{bmatrix} 1 & 0 & 0 \\ 0 & \cos\phi & -\sin\phi \\ 0 & \sin\phi & \cos\phi \end{bmatrix} \tag{5}$$

The transformed coordinates are then used to interpolate the generic field on the neighbour patch. Interpolated scalar fields are assigned to the master patch as-is, while vector fields require an additional transformation, which is performed by the inverse of the rotation matrix.

$$\boldsymbol{v} = \boldsymbol{R}^{-1}\boldsymbol{v}' \,, \tag{6}$$

where $\boldsymbol{v}'$ is the interpolated vector field on the neighbour patch. The field mapping procedure just discussed is employed to map velocity, pressure, turbulent kinetic energy, and the specific rate of dissipation of kinetic energy from the outlet patch to the inlet one. At the outlet, pressure is in turn mapped from the inlet patch, while keeping fixed its surface mean value. To ensure numerical stability a zero-gradient condition is imposed at the outlet for velocity.

3.3. Spatial discretization

The numerical solution of the governing equation is attained by means of a SIMPLE-based Finite Volume solver, implemented in the OpenFOAM computational library [6]. Spatial discretization of advective terms is addressed with second-order upwind schemes. Instead, diffusive terms are discretized by means of central schemes featuring explicit non-orthogonality correction.

Three computational models containing respectively one, two and four channel steps are generated to study the dependency of local and global results on the number of considered channel steps. In order to ensure a correct comparison the three computational domains are discretized with hybrid meshes featuring identical topology: the mesh of the four-slot geometry is

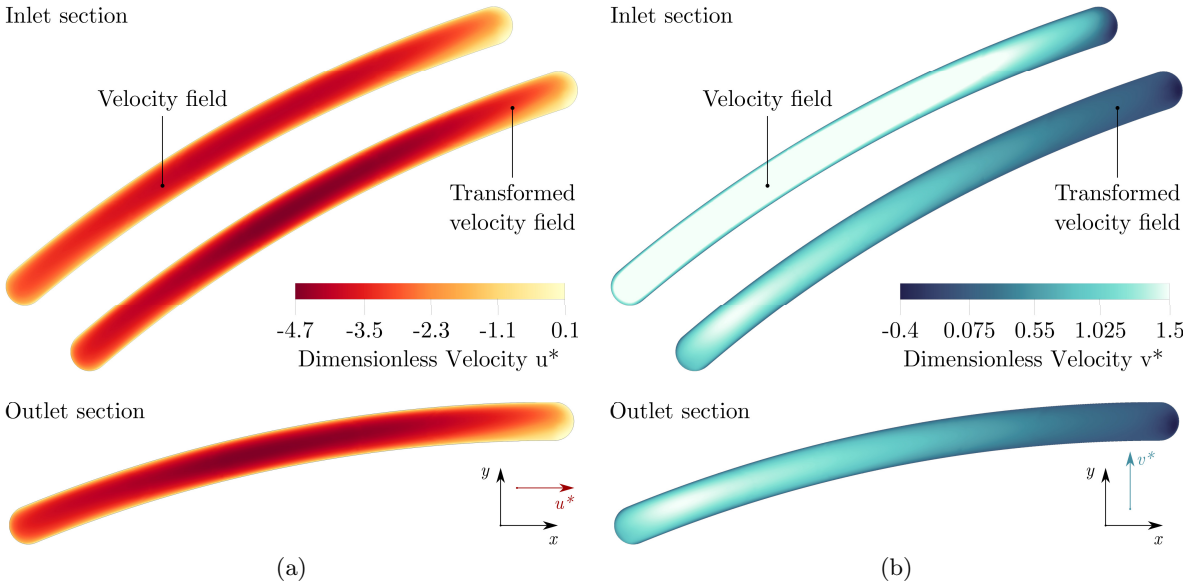

Figure 3. Colour maps of the unchanged and transformed planar components of dimensionless velocity u^* (a) and v^* (b), realised on the inlet and outlet sections.

taken as a starting point, since it is the one with the most complex topology due to the presence of a higher number of fillet radii, then the computational grids of the other two geometries are obtained by deleting the excess channel steps from the four-slots mesh. Figure 2 shows a picture of the computational grid of the two-slot geometry, in which the inlet and outlet patches are highlighted.

3.4. Validation of rototranslational mapping

The explicit mapping procedure developed in this work is validated by performing a preliminary CFD analysis, with the aim of assessing the correct solution coupling between the inlet and outlet sections. To this end, the in-plane velocity components on the inlet and outlet faces, related to a Re=500 flow about two channel steps, are examined. This allows us to evaluate whether scalar fields are mapped correctly and if the rotation transformation is properly applied to the velocity field. In this case the link between the inlet and outlet velocity fields consists of a simple rotation of $2\,\alpha$ around the z axis.

$$\begin{bmatrix} u_{\mathrm{o}} \\ v_{\mathrm{o}} \\ w_{\mathrm{o}} \end{bmatrix} = \begin{bmatrix} \cos(2\,\alpha) & -\sin(2\,\alpha) & 0 \\ \sin(2\,\alpha) & \cos(2\,\alpha) & 0 \\ 0 & 0 & 1 \end{bmatrix} \begin{bmatrix} u_{\mathrm{i}} \\ v_{\mathrm{i}} \\ w_{\mathrm{i}} \end{bmatrix} \tag{7}$$

Figure 3 shows colour maps of the planar dimensionless velocity components on the inlet and outlet sections, furthermore inlet velocity is transformed according to Eq. (7), and displayed on the inlet face. Clearly the coupling of the solution is successful, as the components of the transformed inlet velocity and the outlet one appear identical for both in-plane components, suggesting the correct implementation of the mapping and interpolation schemes, along with the correct application of the geometric transformation. Correct coupling of the solution was verified for all fields, including pressure and turbulence-related quantities.

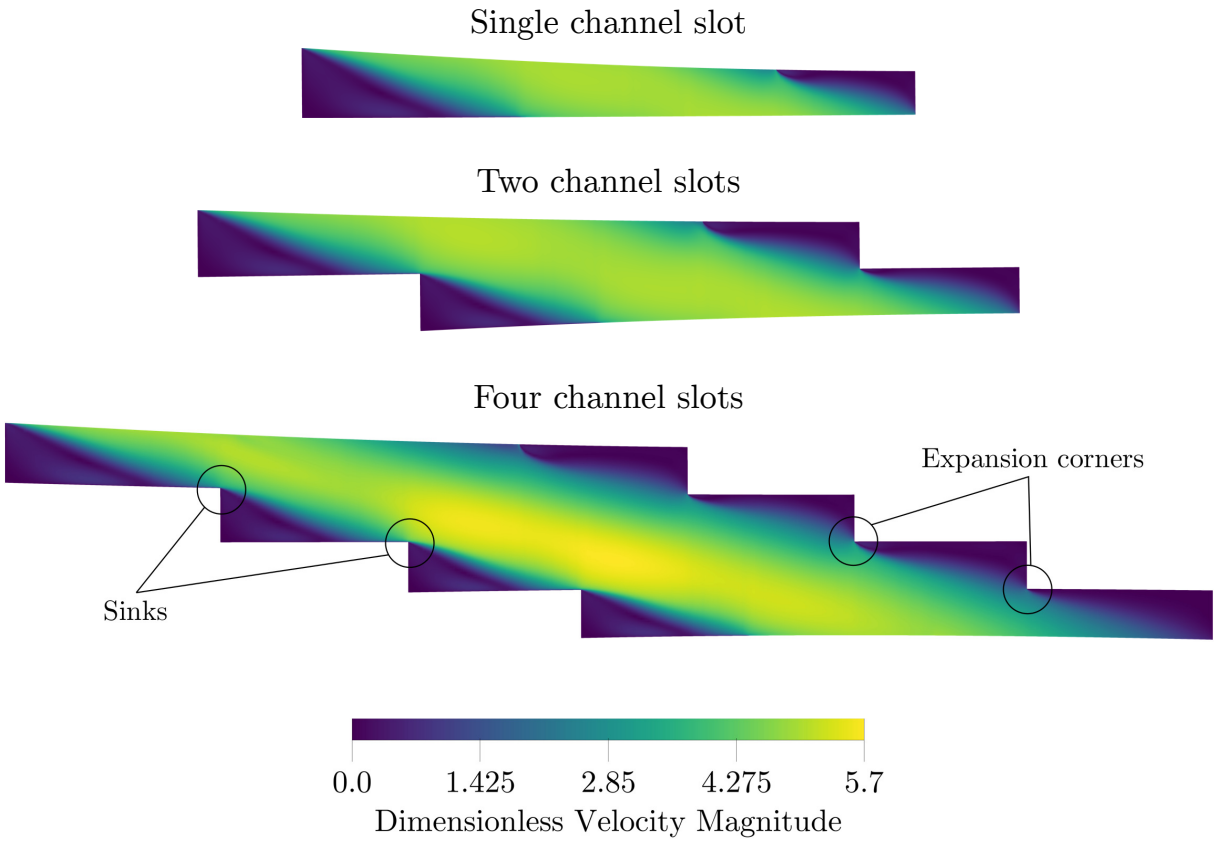

Figure 4. Colour maps of dimensionless velocity magnitude at Re=500 on centred cylindrical sections, of the computational domains that include one (top), two (middle), and four (bottom) channel steps.

3.5. Sensitivity to domain size

Although the numerical solution has been correctly coupled between the inlet and outlet patches, the sensitivity of the results with respect to the number of channel steps must still be investigated, to verify the possible presence of periodic flow structures with a large period, and to evaluate the effects of the zero-gradient condition imposed on the velocity field at the outlet. To this end, three CFD analyses of three different geometries composed respectively of one, two and four channel steps are carried out.

In the following, the sensitivity of results with respect to the number of channel steps is assessed by comparing flow field and integral results. Figure 4 shows three centered cylindrical sections, one for each tested geometry, displaying colour maps of dimensionless velocity magnitude. A careful analysis of the velocity fields reveals that the flow associated to the models containing two and four slots does not repeat perfectly along the different slots: subtle differences can be noticed, particularly by looking at the separation regions located near the expansion corners. In addition, the four-step geometry features high velocity regions near the centre of the channel module, that are not present in the other two solutions. At this point, it is difficult to establish whether the small differences found as a result of the qualitative analysis of the velocity fields are due to flow structures actually present in reality, or to the use of the zero-gradient condition for outlet velocity; nevertheless, the latter is essential to ensure numerical stability of the developed method.

A first analysis on the variation of head losses as a function of the number of channel steps

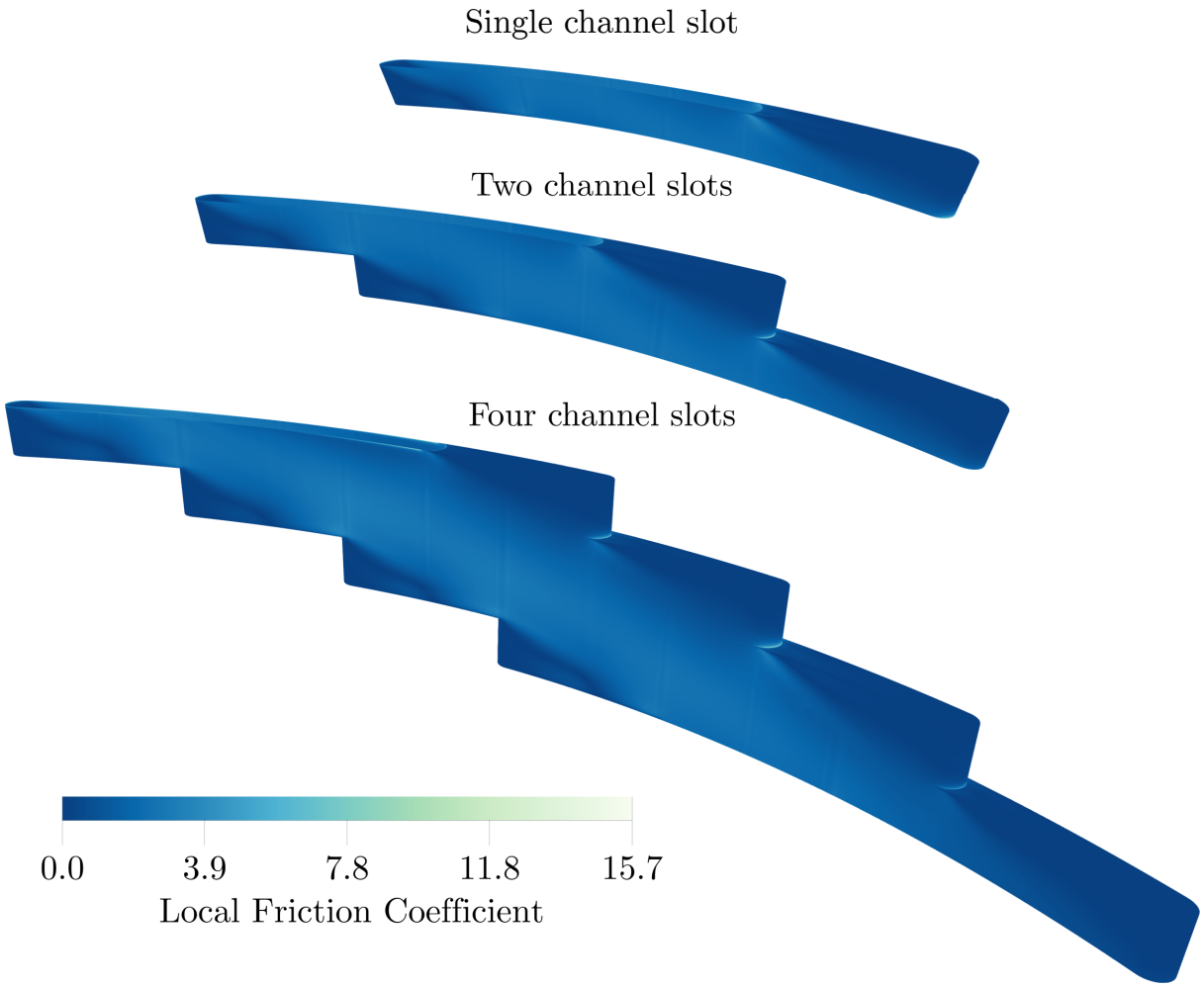

Figure 5. Distributions of local friction coefficient at Re=500 of three periodic modules, made up of one (top), two (middle), and four (bottom) channel slots.

considered is done by examining the distribution of the local friction coefficient on the channel walls, which is shown in Fig. 5, for the three computational domains. Also in this case, subtle differences among the three solutions can be spotted near the expansion corners, however these are less marked with respect to the ones encountered in the analysis of the velocity field, meaning that the head losses values computed with the three models should be similar. This is confirmed by the global results on head losses which are shown in the following. Integral results on head losses are presented by means of an equivalent Darcy friction factor, which is computed according to the Darcy–Weisbach equation, considering the height of the single channel step y as the reference length, and expressing the pressure gradient on the basis of the arc length of the cylindrical helix formed by the slots:

$$f = \frac{2\,\sigma\,y^2}{\rho\,\bar{w}_{\mathrm{i}}^2 \alpha \sqrt{r^2 + y^2/\alpha^2}}\,. \tag{8}$$

In Eq. (8) σ is the external forcing term resulting from the CFD analyses, while $\bar{w}_{\mathrm{i}}^2$ is the surface mean of the velocity component normal to the inlet section. The friction factor values obtained for the three geometries, together with their relative deviations are reported in Tab 1.

These results are very promising, as f is in fact nearly independent of the number of channel steps included in the computational model. This is in agreement with the previously discussed local results.

The obtained results demonstrate that, although the developed numerical method does not allow for the achievement of perfect fully developed flow conditions, this does not significantly affect local and global results on head losses, which are the main focus of this study. For this reason, the computational model made up of a single channel step is chosen for all the following analyses.

3.6. Mesh sensitivity analysis

Grid dependence of integral results is investigated by comparing friction factor values obtained from three computational meshes of a single channel step. The coarse and fine grids are constructed by doubling and halving the size of the reference element of the base mesh, which was also used for all the previous analyses. These three computational grids feature the same exact topology.

Table 2 reports f-values obtained for three single slot meshes, along with the dimensionless size of the reference element, and surface mean dimensionless wall distance. The resulting friction factor values are within 1.5% of each other, furthermore they are not convergent with respect to mesh resolution. In all three cases the mean y^+ value is well below unity, which is consistent with the selected wall treatment. The base mesh is retained for the following CFD analyses, since the mesh sensitivity study did not highlight a convergent behavior; besides, the sensitivity of the results with respect to grid size and number of channel steps are of the same order of magnitude.

4. Results

A first study on the head losses associated with the cooling channels is performed by carrying out several CFD analyses at different Re-values. The resulting values of the equivalent Darcy friction factor, computed according to Eq. (8), are employed to derive a correlation function based on the Reynolds number:

$$f = -2428\ \mathrm{Re}^{0.00026} + 2434\ . \tag{9}$$

Table 1. Friction factor values obtained from the computational models having one, two, and four channel steps.

Number of channel steps	f	Difference to previous model
1	2.072	-
2	2.078	0.29%
4	2.064	-0.66%

Table 2. Friction factor and mean dimensionless wall distance values obtained from the coarse, medium, and fine computational meshes of a single channel step.

Grid	Δ^*	$\bar{y}^+$	f	Difference to previous grid
Coarse	0.1	0.90	2.104	-
Base	0.05	0.48	2.072	-1.53%
Fine	0.025	0.24	2.098	1.25%

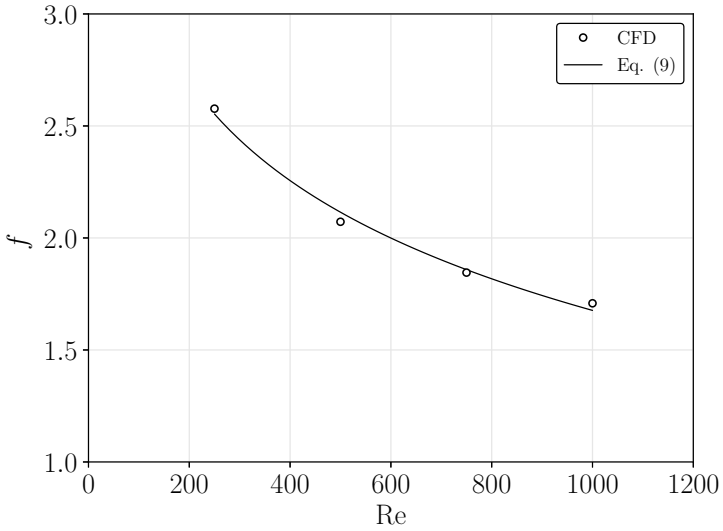

Figure 6. Numerical results and the associated correlation for the equivalent Darcy friction factor.

The plot of Fig. 6 reports the numerically obtained f-values as well as the graph of Eq. (9): as expected, given the low Re-values considered, the friction factor decreases with growing Re.

Overall head losses related to the cooling jacket are computed by means of the Darcy-Weisbach formula considering the following set of hypotheses: (i) the flow is assumed isothermal, thus fluid properties remain constant along the channels; (ii) entrance effects and the contribution to head losses given by the manifolds, which distribute the flow across the channels are neglected; (iii) the flow is equally distributed among the six cooling channels.
The total pressure drop is given by:

$$\Delta p_{\mathrm{T}} = \frac{1}{2}\,\rho\, f\, \frac{L_{\mathrm{h}}}{y}\,\bar{w}_{\mathrm{i}}^{\,2}\,, \tag{10}$$

where L_{h} is the arc length of the cylindrical helix identified by a channel, and it is computed from the line integral of Eq. (1), and by expressing the total swept angle as a function of the offset angle between two channel slots α, and the total number of plates n constituting the motor casing.

$$L_{\mathrm{h}} = n\,\alpha\sqrt{r^{\,2} + y^{\,2}/\alpha^{\,2}} \tag{11}$$

At a flow rate of 10 l/min of a water-glycol solution the total pressure drop referred to an arc length of 595 mm amounts to 4.03 mbar, which is within the expected range of values for this type of cooling jacket. Obviously this and previous results must be taken as preliminary, since experimental tests, necessary for the validation of the proposed methodology, have not been performed yet.

5. Concluding remarks

This work discussed the numerical analysis of the cooling jacket of an electric motor with a particular focus on head losses. In an effort to reduce the required computational cost, cooling channel were studied by means of periodic modules analysed under fully developed flow conditions. The rototranslation transformation associated with the inlet and outlet sections required the development of novel CFD tools, to achieve the coupling of the numerical solution between the inlet and outlet sections of the cooling channels. The newly developed tools were

validated by performing a test CFD run. Subsequently, numerical analyses of domains including one, two, and four channel steps were performed, in order to determine the dependence of results on the number of periodic units considered. The results shown that for the considered geometry head losses are basically independent of the number of channel steps included in the computational domain; on the other hand, this analysis highlighted a weakness of the proposed method: the zero-gradient condition imposed, for stability reasons, on velocity at the outlet does not allow for the obtainment of perfect fully developed flow conditions; although, this does not seem to have a strong influence on the resulting head losses values.

The smallest periodic module, consisting of a single channel step, was chosen to perform the grid sensitivity analysis and to obtain a suitable correlation for the equivalent Darcy friction factor. Finally, the aforementioned correlation was employed in conjunction with the Darcy Weisbach formula to retrieve a first estimation of the total head losses related to the cooling jacket.

The numerical approach developed in this work can be applied for the analysis of any problem which requires the coupling of the numerical solution between rototranslated mesh faces. Although the work done so far can be viewed as a good starting point, numerical stability problems are a concern, and they will be tackled by devising an implicit formulation for the developed boundary condition, as part of future research efforts. Other lines of development could include the implementation of dedicated numerical codes to be able to address the problem in cylindrical or helical coordinates, which would eliminate the need to apply rotation transformations to vector fields.

The study of the cooling jacket examined in this work will be extended by carrying out a complete analysis of heat transfer performance, and present and future results will be extended over a wider range of flow regimes.

Acknowledgments

The research has been partially funded under the National Recovery and Resilience Plan (NRRP), Project "Sustainable Mobility Center (Centro Nazionale per la Mobilità Sostenibile - CMNS)", Project code CN00000023 - CUP E93C22001070001.

References

[1] Deisenroth D C and Ohadi M Thermal management of high-power density electric motors for electrification of aviation and beyond 2019 *Energies* **12**

[2] Ye Z n, Luo W d, Zhang W m and Feng Z x 2011 Simulative analysis of traction motor cooling system based on cfd *2011 International Conference on Electric Information and Control Engineering* pp 746–749

[3] Pechánek R and Bouzek L 2012 Analyzing of two types water cooling electric motors using computational fluid dynamics *2012 15th International Power Electronics and Motion Control Conference (EPE/PEMC)* pp LS2e.4–1–LS2e.4–5

[4] Nategh S, Huang Z, Krings A, Wallmark O and Leksell M Thermal modeling of directly cooled electric machines using lumped parameter and limited cfd analysis 2013 *IEEE Transactions on Energy Conversion* **28** 979–990

[5] Ponomarev P, Polikarpova M and Pyrhönen J 2012 Thermal modeling of directly-oil-cooled permanent magnet synchronous machine *2012 XXth International Conference on Electrical Machines* pp 1882–1887

[6] Weller H G, Tabor G, Jasak H and Fureby C A tensorial approach to computational continuum mechanics using object-oriented techniques 1998 *Computers in Physics* **12** 620–631

[7] Menter F Two-equation eddy-viscosity turbulence models for engineering applications 1994 *AIAA Journal* **32** 1598 – 1605